Bayesian estimation of tension in bridge hangers using modal frequency measurements

Costas Papadimitriou[*1], Konstantina Giakoumi[1a], Costas Argyris[1b],
Leonidas A. Spyrou[2c] and Panagiotis Panetsos[3d]

[1]*University of Thessaly, Department of Mechanical Engineering, Volos 38334, Greece*
[2]*Centre for Research and Technology Hellas (CERTH), Institute for Research and Technology - Thessaly,
Volos 38333, Greece*
[3]*Egnatia Odos S.A., Capital Maintenance Department, Thermi 57001, Greece*

Abstract. The tension of an arch bridge hanger is estimated using a number of experimentally identified modal frequencies. The hanger is connected through metallic plates to the bridge deck and arch. Two different categories of model classes are considered to simulate the vibrations of the hanger: an analytical model based on the Euler-Bernoulli beam theory, and a high-fidelity finite element (FE) model. A Bayesian parameter estimation and model selection method is used to discriminate between models, select the best model, and estimate the hanger tension and its uncertainty. It is demonstrated that the end plate connections and boundary conditions of the hanger due to the flexibility of the deck/arch significantly affect the estimate of the axial load and its uncertainty. A fixed-end high fidelity FE model of the hanger underestimates the hanger tension by more than 20 compared to a baseline FE model with flexible supports. Simplified beam models can give fairly accurate results, close to the ones obtained from the high fidelity FE model with flexible support conditions, provided that the concept of equivalent length is introduced and/or end rotational springs are included to simulate the flexibility of the hanger ends. The effect of the number of experimentally identified modal frequencies on the estimates of the hanger tension and its uncertainty is investigated.

Keywords: structural identification; Bayesian inference; model selection; uncertainty quantification; hanger tension; structural safety

1. Introduction

Hangers are used as deck support elements in arch bridges. Methods to monitor the axial loads in hangers are important for identifying the structural integrity of arch bridges. Large enough axial loads in the hangers affect the hanger modal frequencies due to the stiffness increase, so that the

---

*Corresponding author, Professor, E-mail: costasp@uth.gr
[a] Undergraduate Student, E-mail: dina.giakoumi@gmail.com
[b] Ph.D. Student, E-mail: koargiri@uth.gr
[c] Ph.D., E-mail: lspyrou@ireteth.certh.gr
[d] Ph.D., E-mail: ppane@egnatia.gr

estimation of the axial load can be based on comparing model predictions with the experimentally estimated modal frequencies. The axial load is then estimated as the one that gives model predictions of the modal frequencies that matches the experimentally identified modal frequency values. The model predictions of the modal frequencies are affected by the flexural rigidity, end connection details and boundary conditions at the end supports of the hangers. Connections of a circular cross-section hanger to the bridge deck and arch may often be made through metallic guides or plates and give rise to boundary conditions that are not well defined, complicating the selection of the appropriate boundary conditions in a modeling procedure (Lagomarsino and Calderini 2005). Depending on the connections, the arch or the deck may be flexible in different direction of motion. To obtain reliable predictions of the hanger axial loads these factors should be taken into account in the modeling.

Methods based on string and beam theory (Bokaian 1990, Barcilon 1976) have been developed for estimating the cable tension from experimentally identified modal frequencies. Exact formulas requiring the iterative solution of the characteristic equation as well as simplified practical formulas have been proposed for the estimation of the tension (Zui, Shinke *et al.* 1996, Fang and Wang 2012, Ren, Chen *et al.* 2005, Nam and Nghia 2011, Huang, Fu *et al.* 2015) taking into account the bending stiffness and sag-extensibility. To account for the boundary conditions, Ceballos and Prato (2008) introduced rotational springs at the cable ends. Techniques were introduced to approximately determine the rotational spring stiffnesses and the axial force and cable bending stiffness were then adjusted to fit the experimental values of the modal frequencies. The problem of tension estimation in tie-rods using beam theory and rotational springs to simulate unknown boundary conditions was also discussed in Lagomarsino and Calderini (2005). Bellino, Marchesiello *et al.* (2010) has introduced the concept of equivalent cable length to account for the unknown boundary conditions. They proposed a method to estimate the cable tension by means of vibration response and moving mass technique. The same authors (Bellino, Garibaldi *et al.* 2011) introduced the modal length concept and developed a method for estimating the cable tension using supplementary measurements from a cable with an added mass. Belleri and Moaveni (2015) have also used the concept of equivalent length and rotational springs to account for uncertain boundary conditions, providing reliable estimates of tensile loads in tie rods using measurements of the first modeshape in addition to the modal frequency measurements.

FE modeling of the hanger was also used to accurately identify the hanger tension, flexural and axial rigidity. A FE model can be used as a baseline model for identifying the cable tension (Kim and Park 2007). The importance of boundary conditions on the reliable estimates of the modal frequencies from a FE model was pointed out in Park, Seong *et al.* (2015). Ni, Ko *et al.* (2010) used FE modeling to estimate the cable tension from multimodal measurements, concluding that for long-span large-diameter cables the tension is reliably estimated when accurately accounting for all effects such as bending stiffness, boundary conditions as well as other constraints. The construction of a finite element model requires special software and resources and may be a time consuming procedure, especially when solving the inverse problem of estimating the cable tension and boundary conditions. Simple models based on beam theory that include the effect of flexural rigidity, flexibility due to end connections and boundary conditions can provide computationally inexpensive estimates of the hanger tension.

The objective of this work is to estimate the hanger tension in relatively large-diameter hangers of arch bridges that are connected to the bridge deck and arch through sizable metallic end plates, asymmetrically oriented at bottom and top hanger ends, making difficult the specification of the cable length, hanger-plate assembly flexibility and boundary conditions. The estimation is based

on modal frequencies of the cable, in both the longitudinal and transverse direction of the bridge, identified from modal tests. Two different categories of model classes are introduced to represent the dynamics of the hanger. Different model classes in both categories are used to predict the hanger modal frequencies given the axial load in the hanger. The first category is based on a conventional analytical beam model formulation resulting from Euler-Bernoulli beam theory, used to predict the modal frequencies of the hanger with various boundary conditions, given the tension on the hanger. Two sets of boundary conditions are considered, one with fixed ends and the other with flexible ends, quantified by rotational springs attached at the ends. The concept of the equivalent length that is left free to be estimated together with the hanger tension so that predictions match the measurements is also considered. Analytical transcendental equations are developed and numerically solved to obtain the modal frequencies.

The second category is based on high-fidelity three-dimensional baseline FE models developed in Abaqus for the hanger, including the end plate connections. Two different types of boundary conditions are implemented and the effect on the hanger tension estimation is evaluated. The first type assumes fixed ends, while the second type models the end surfaces that connect to the deck and the arch as flexible with respect to the rotation about axes perpendicular to the hanger axis. The flexibility of the end supports arises from the flexibility of the arch and the deck at the connection ends and is appropriately modeled by attaching on the boundary plate ends a set of distributed springs along the direction of hanger axis to simulate the rotation along the two axes perpendicular to the hanger axis. The procedure for predicting the modal frequencies from the FE models given the hanger tension and the boundary conditions is outlined.

Bayesian inference (Beck and Katafygiotis 1998, Yuen 2010) for parameter estimation and model selection is used for estimating the hanger tension based on the different model classes introduced and the experimentally identified modal frequencies. The Bayesian model selection method (Beck and Yuen 2004) is used to select the best model class for representing the dynamics of the hangers. In contrast to existing methods, the present work uses Bayesian inference for the first time to discriminate between model classes, select the best model class out of a series of increasingly complex models, as well as estimate the axial force and its uncertainty. The present investigation includes comparison of results and conclusions related to the estimate of the hanger tension along with its uncertainty, the effect of the number of experimental frequencies available from modal tests, the effect of end plate connections and boundary conditions on the prediction of the hanger tension, as well as the adequacy of each one of the model class to represent the dynamics of the hanger.

The presentation in this paper is organized as follows. Section 2 gives a detailed description of the hanger and the experimental data available. Section 3 introduces the modal frequency prediction approach based on the Euler-Bernoulli beam theory. Section 4 presents details for the prediction of the modal frequencies using high fidelity FE models of the hanger with fixed and flexible support conditions. Section 5 briefly presents the Bayesian inference tools for model selection and parameter estimation. Section 6 presents the results of the hanger tension estimation applying the Bayesian inference framework on the different model classes. Conclusions are presented in Section 7.

2. Description of hanger and experimental data

The hanger under investigation is hanger 3 of the 20 hangers used to support the deck of an

352   *Costas Papadimitriou et al.*

arch bridge located in Athens, Greece. The arch bridge is shown schematically in Fig. 1. The hanger geometry, along with the geometry of the connections of the hangers to the deck and the arch, is shown in Fig. 2(a). The hangers are made out of steel and they are connected to the deck and the arch substructures with edge plates as shown in Fig. 2(b). The edge plates are welded to the hangers and deck or the arch. The connections of the hanger with the deck or the arch with end plates are approximately 1 m long and affect the hanger flexibility at the two ends. The plate that connects the hanger with the deck has its orientation along the longitudinal direction of the bridge deck, while the plate that connects the hanger to the arch has its orientation along the transverse direction of the bridge deck. The boundary conditions at the plate surface that connects to the arch or the deck substructures depend on the flexibility of the deck and the arch.

The hangers are made of steel with modulus of elasticity $E = 200 GPa$, mass density 7800 kg/m^3 and Poisson ratio 0.3. The total length of the hanger 3 including the connections is 12 m, while the clear length of the circular section of the hanger is 9.817 m. The diameter of the circular section of the hanger is 0.13 m.

It should be noted that the hanger differs from conventional cables which are often assumed as string elements. The bending stiffness of the present hanger cannot be ignored in predicting the modal frequencies. In addition the plate elements installed in the hangers to connect the circular section to the bridge arch and deck also affect the bending stiffness.

Based on the design plans, the geometry of the hanger, its material properties and the connection details of the two edge plates of the hanger are identical. The only difference is the orientation of each edge plate. Assuming that the end conditions of the edge plates are fixed, the modal frequencies of vibration of the hanger along the longitudinal and transverse direction bridge are expected to be identical.

Impulse hammer tests performed on the hanger 3 of the bridge are used to estimate the modal frequencies of the hanger. The tests are performed using two acceleration sensors placed on the hanger at distances approximately 1.9 m to 2.3 m from its bottom edge. The sensor configuration is such that one acceleration sensor measures along the longitudinal direction and the other along the transverse direction of the bridge. To avoid placing sensors close to a node of a mode shape, two sensor setups are used, one with both sensors placed at approximately 2.3 m from the bottom edge of the hanger and the other with both sensors placed at approximately 0.4 m lower than the first location. For each set up, two impulse hammer tests are performed, one striking the hammer on the hanger along the longitudinal and the other striking the hanger along the transverse direction of the bridge, ensuring that the hanger modes along the longitudinal and transverse directions are excited, respectively. The impact locations of the hammer are chosen to be in close proximity to the location of the sensors. For each setup and test case, the measurements consist of the time histories of the hanger force and the two accelerations. Two sets of measurements are available to identify each mode. For each set of measurements, the optimal values of the lowest six modal frequencies in either the longitudinal or the transverse directions are estimated using nonlinear least-squares frequency domain methods, minimizing the Euclidean norm of the difference between the experimentally identified frequency response functions estimated by the measured time histories and the ones predicted by a modal model of the hanger (Heylen, Lammens *et al.* 1995, Ewins 2000).
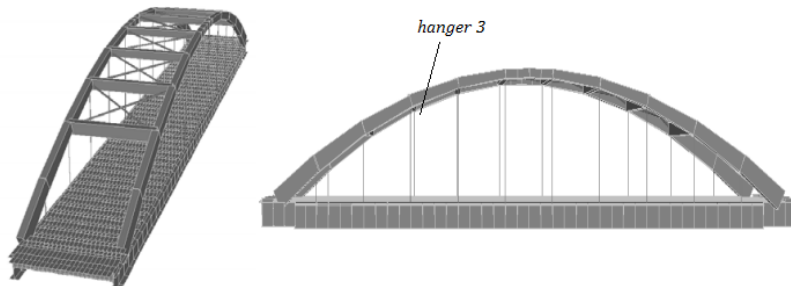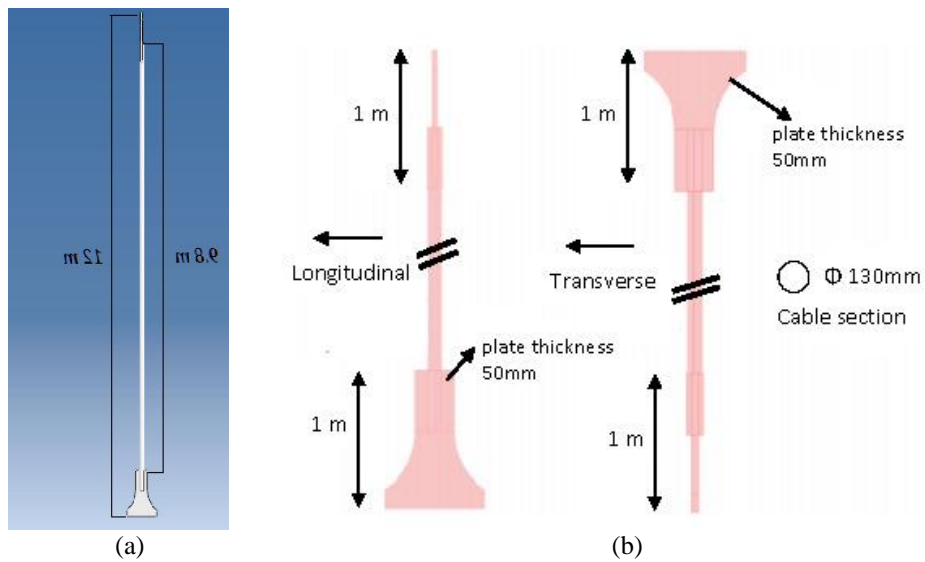
Fig. 1 The arch bridge

| (a) | (b) |

Fig. 2 (a) The geometry of hanger 3 and (b) The geometry of the plates connecting the circular hanger to the arch and the deck of the bridge

Table 1 Experimentally identified modal frequencies (Hz) of hanger 3 in the transverse (trans) and longitudinal (long) directions

Mode #	trans	long	% difference
1	5.82	6.09	2.3
2	13.85	14.8	3.3
3	26.17	27.0	1.6
4	40.47	41.8	1.6
5	59.3	61.5	2.8
6	81.3	83.68	1.4

Table 1 shows the optimal values of the experimentally identified modal frequencies of hanger 3 in the transverse and longitudinal directions. Note that the uncertainty in the experimentally identified values of the modal frequencies are not reported due to the small number of experimental tests available. However, they are expected to be considerably less than 1%. It is observed that the modal frequencies differ in the two longitudinal and transverse directions. The percentage differences range from 1.4% to 3.3% and cannot be justified by material or geometric variability of the hanger. Due to the symmetry of the hanger and the connection plates, this is a strong indication that the boundary conditions at the end of the hangers are responsible for such differences. Thus the hanger end conditions cannot be assumed to be fixed. This study investigates the effects of the boundary conditions on the estimation of the axial force and provides evidence, based on Bayesian inference, that fixed boundary conditions assumed for the ends may result in misleading estimates of the axial hanger loads.

3. Modal frequency predictions based on beam theory

The prediction of the modal frequencies of the hanger subjected to an axial load is based on the Euler-Bernoulli beam theory. The equation of motion of a beam subjected to axial tension T along the beam axis z is given by (William 1996)

$$EI \frac{\partial^4 u}{\partial^4 z} - T \frac{\partial^2 u}{\partial^2 z} + \rho A \left(\frac{\partial^2 u}{\partial t^2} \right) = 0 \tag{1}$$

where $u \equiv u(z,t)$ is the deflection of the beam in a direction y in the (y,z) plane, ρ is the density, E is the modulus of elasticity, I is the moment of inertia of the circular cross section about the x and y axes, and A is the area of the cross-section of the beam. All geometrical and material properties are assumed constant along the length of the beam.

Two models are introduced that differ on the boundary conditions considered. In the first model the ends of the beam are fixed, whereas in the second model the ends are flexible. The flexibility in rotation of the ends is simulated using rotational springs.

3.1 Beam with fixed ends

For fixed-end supports, the boundary conditions are $u(0,t) = 0$, $u(L,t) = 0$, $u'(0,t) = 0$, $u'(L,t) = 0$. Following the usual eigenvalue analysis, the modal frequencies are obtained by solving the characteristic equation

$$h(\gamma, \zeta) = det \begin{pmatrix} 0 & 1 & 0 & 1 \\ bl & -c_{22}bl & al & c_{24}al \\ sinh(bl) & cosh(bl) & sin(al) & cos(al) \\ c_{41}blcosh(bl) & c_{42}blsinh(bl) & c_{43}alcos(al) & -c_{44}alsin(al) \end{pmatrix} = 0 \tag{2}$$

where al and bl are given as

$$al = l\sqrt{\sqrt{\zeta^4 + \gamma^4} - \zeta^2}, \quad bl = l\sqrt{\sqrt{\zeta^4 + \gamma^4} + \zeta^2} \tag{3}$$

with respect to the two parameters γ and ζ defined by

$$\gamma^4 = \frac{m\omega^2}{EI}, \quad \zeta = \sqrt{\frac{T}{2EI}} \tag{4}$$

and $m = \rho AL$ is the mass of the beam. The elements c_{ij} are given in this case by $c_{22} = c_{24} = 0$ and $c_{41} = c_{42} = c_{43} = c_{44} = 1$. Eq. (2) can also be written as (Zui, Shinke *et al.* 1996)

$$2(al)(bl)[1 - cos(al)cos(bl)] + [(bl)^2 - (al)^2]sin(al)sinh(bl) = 0 \tag{5}$$

The problem of estimating the modal frequency ω in Eq. (2) or Eq. (5) given the axial force T is turned into the problem of estimating γ given the value of ζ. The values of γ can be obtained by the numerical solution of Eq. (2) or Eq. (5).

To proceed, the following dimensionless parameter

$$\xi = \sqrt{\frac{T}{EI}} l \tag{6}$$

is introduced due to its significant role (Zui, Shinke *et al.* 1996) in the dynamic behavior of the beam. For large values of ξ ($\xi \geq 20$) the dynamic characteristics of the beam are similar to those of a string. For small values of ξ ($\xi < 20$), the characteristics of a hanger are similar to those of a beam. Two different parameterizations have been proposed (Zui, Shinke *et al.* 1996) depending on the range of ξ values.

For large values of ξ ($\xi \geq 20$), the dimensionless parameter

$$\eta_n = \frac{f}{f_n^s} \tag{7}$$

is introduced, where

$$f_n^s = \frac{n}{2l}\sqrt{\frac{Tg}{w}} \tag{8}$$

is the theoretical values of the n-th order natural frequency ($\omega = 2\pi f$) of a string (Humar 2001). In this case al and bl in Eq. (3) take the form

$$al = \frac{\xi}{\sqrt{2}}\sqrt{-1 + \sqrt{1 + \left(\frac{2n\pi\eta_n}{\xi}\right)^2}} \quad bl = \frac{\xi}{\sqrt{2}}\sqrt{1 + \sqrt{1 + \left(\frac{2n\pi\eta_n}{\xi}\right)^2}} \tag{9}$$

while the characteristic Eq. (5) becomes

Table 2 The first six roots of $cos(a)cosh(a) = 1$

a_1	a_2	a_3	a_4	a_5	a_6
4.73	7.8532	10.9956	14.1372	17.2788	20.4204

$$g(\eta_n, \xi) = 2n\pi\eta_n(1 - cos(al)cosh(bl)) + \xi sin(al)sinh(bl) = 0 \qquad (10)$$

where, using Eqs. (4), (6), (7) and (8), the function $g(\eta, \xi) = h(\sqrt{n\pi\xi\eta} / l, \xi / (l\sqrt{2}))$ with $h(\gamma, \zeta)$ defined in Eq. (2). The normalized modal frequencies η_n are obtained by solving the characteristic Eq. (10) for a given value of ξ.

For small values of ξ ($\xi < 20$), the dimensionless parameter

$$\varphi_n = \frac{f}{f_n^b} \qquad (11)$$

is introduced, where

$$f_n^b = \frac{a_n^2}{2\pi l^2}\sqrt{\frac{EIg}{w}} \qquad (12)$$

is the theoretical value of the n-th order natural frequency of a beam fixed at both ends (Humar 2001). The values of a_n are the solutions of $cos(a)cosh(a) = 1$. The first six solutions are given in Table 2.

In this case al and bl in Eq. (3) are transformed into

$$al = \frac{\xi}{\sqrt{2}}\sqrt{-1 + \sqrt{1 + \left(\frac{2\alpha_n^2}{\xi^2}\varphi_n\right)^2}}, \quad bl = \frac{\xi}{\sqrt{2}}\sqrt{1 + \sqrt{1 + \left(\frac{2\alpha_n^2}{\xi^2}\varphi_n\right)^2}} \qquad (13)$$

while the characteristic equation takes the form

$$g(\varphi_n, \xi) = 2a_n^2\varphi_n(1 - cos(al)cosh(bl)) + \xi^2 sin(al)sinh(bl) = 0 \qquad (14)$$

where, using Eqs. (4), (6), (11) and (12), the function $g(\eta, \xi) = h(\alpha_n\sqrt{\eta} / l, \xi / (l\sqrt{2}))$ with $h(\gamma, \zeta)$ defined in Eq. (2). The normalized modal frequencies φ_n are obtained by solving Eq. (14) for a given value of ξ. When the axial force approaches zero ($\xi = 0$) then φ_n tends to 1.

3.2 Beam with flexible ends

For flexible supports, modeled by rotational springs at the two ends as shown in Fig. 3, the boundary conditions for beam deflections in the (y, z) plane are $u(0, t) = 0$,

$EIu''(0,t) - k_1u'(0,t) = 0$, $u(\mathrm{L},t) = 0$ and $EIu''(L,t) + k_3u'(L,t) = 0$, where k_1 and k_3 are the rotational springs applied at the ends (Fig. 3(a)) to resist rotation around x direction due to bending. Similar support conditions hold for beam displacements in the (x,z) plane with k_2 and k_4 introduced as rotational springs applied at the ends (Fig. 3(b)) to resist rotations with respect to the y direction. The prediction of the axial force is obtained by solving the characteristic equation for the flexible boundary conditions represented by rotational springs (Lagomarsino and Calderini 2005). Ceballos and Prato (2008) have derived explicit expressions which are required to be solved iteratively. Next we briefly state the characteristic equation.

Introducing the following dimensionless parameters for the spring constants

$$k_a = \frac{k_1 l}{EI} \quad \text{and} \quad k_c = \frac{k_3 l}{EI} \tag{15}$$

and following the usual eigenvalue analysis, the modal frequencies in the (y,z) plane are obtained by solving the characteristic Eq. (2), where the elements c_{ij} are given in this case by

$$c_{22} = \frac{bl}{k_a}, \quad c_{24} = \frac{al}{k_a} \tag{16a}$$

$$c_{41} = 1 + \frac{(bl)}{k_c} tanh(bl), \quad c_{42} = 1 + \frac{(bl)}{k_c} \frac{1}{tanh(bl)} \tag{16b}$$

$$c_{43} = 1 - \frac{(al)}{k_c} tan(al), \quad c_{44} = 1 + \frac{(al)}{k_c} \frac{1}{tan(al)} \tag{16c}$$

Note that for very large values of k_a and k_c, such that the following conditions hold

$$\frac{al}{k_a} << 1, \quad \frac{bl}{k_a} << 1, \quad \frac{al}{k_c}[tan(al)]^{\pm 1} << 1, \quad \text{and} \quad \frac{bl}{k_c}[tanh(bl)]^{\pm 1} << 1 \tag{17}$$

the corresponding elements $c_{22} = c_{24} = 0$ and $c_{41} = c_{42} = c_{43} = c_{44} = 1$ and the characteristic equation tends to the one for the beam with fixed supports. Moreover, for large values of ξ ($\xi >> 20$), say $\xi > 200$ the hanger behaves as a string which means that the flexural stiffness of the hanger is not important and thus the flexibility of the end supports does not affect the modal frequencies.

Similar expression holds for estimating the modal frequencies in the (x,z) plane with k_a and k_c replaced by $k_b = k_2 l / EI$ and $k_d = k_4 l / EI$.

3.3 Estimation of modal frequencies

The lowest seven dimensionless frequencies η_n and φ_n for beam with fixed ends, calculated

from the Eqs. (10) and (14) for large and small values of ξ, are given in Figs. 4(a) and 4(b), respectively. Eqs. (10) and (14) are transcendental equations and for their solution an iterative method can be used such as the Newton-Raphson algorithm. Herein the "fzero" function in Matlab is used. In order to minimize or eliminate the probability of missing the correct solutions for a given ξ value, the procedure of estimating modal frequencies starts from large values of ξ ($\xi > 200$), where the solution approaches the known values given, due to Eqs. (7) and (8), by $\eta_n = n$, $n = 1, 2, \ldots$. Subsequently, the modal frequencies for smaller values $\xi - \delta\xi$ are obtained iteratively using the previous solutions for ξ as an initial estimate to find the zeros of the function $g(\eta, \xi - \delta\xi)$ close to the solutions at $\eta(\xi)$. Using the method described above, Eqs. (10) and (14) have been solved and the values of η or φ are tabulated for values of ξ ranging from [0,700] to be further used for estimating the modal frequencies at the intermediate values of ξ for either fixed or flexible supports as follows.

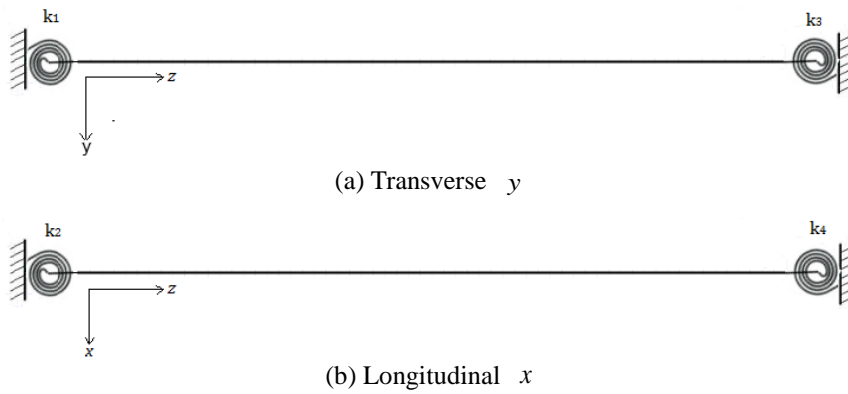(a) Transverse y

(b) Longitudinal x

Fig. 3 The rotational springs resisting rotation of ends about the transverse y and longitudinal x directions
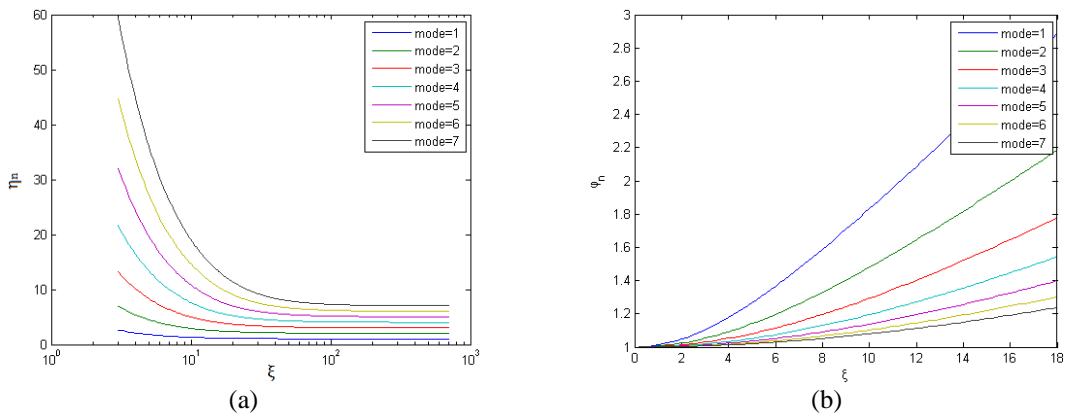

Fig. 4 The dimensionless solutions (a) $\eta_n = n\eta$ versus ξ for large values of ξ, and (b) φ ($\varphi_n = a_n^2 \varphi$) versus ξ for small values of ξ for beam with fixed ends

First, it should be noted that the solution of Eqs. (10) and (14) for fixed ends are upper bounds of the solution of Eq. (10) with flexible ends, since the flexibility at the supports is expected to reduce the values of the modal frequencies for all modes. This observation can be used to construct an algorithm for reliably obtaining the solutions of the modal frequencies of the beam with fixed or flexible supports for any value of $\xi \in [0, 700]$. These solutions are obtained using fsolve or fzero in Matlab by providing the intervals where the solution lies or starting values very close to the solutions. This has to be done with a 100% reliability since this procedure is automated to be used within the Bayesian framework (see Section 5) to compute the solutions for a large number of sample points ξ. To find the lowest k solutions of the transcendental equation $g(\eta, \xi)$ for a fixed value of ξ, the following steps are performed:

1. Given ξ, find i such that $\xi \in [\xi_i, \xi_{i+1}]$ using the tabulated ξ_i values.
2. Estimate $\eta_i = \eta(\xi_i)$ and $\eta_{i+1} = \eta(\xi_{i+1})$ and use linear interpolation to estimate $\eta = \eta(\xi) = \eta(\xi_i) + [\eta(\xi_{i+1}) - \eta(\xi_i)](\xi - \xi_i) / (\xi_{i+1} - \xi_i)$.
3. Divide the interval $[0, (1+a)\eta]$, where $a \ll 1$ is selected by the user, into N equal intervals of size $\Delta\eta = (1+a)\eta / N$. Compute $g_j = g(j\Delta\eta, \xi)$, $j = 1 \ldots, N$.
4. Find the values of η among the $\eta_j = j\Delta\eta$ for which a sign change occurs in the function $g(\eta, \xi)$. The Matlab command η (find(diff(sign(g)) =0) can be used. Let ℓ be the number of sign changes.

   - If $\ell >= k$ select the lowest k values η_j, $j = 1, \ldots, k$ and use each one of these k values as starting value to find the zeros of the function $g(\eta, \xi)$.
   - If $\ell < k$ then go to 3, set $N \leftarrow 2N$ and repeat the steps until an $\ell >= k$.

The algorithm guarantees that the lowest k modal frequencies can be found with a high reliability, provided that $\Delta\eta$ is significantly less than the minimum distance between consecutive roots of $g(\eta, \xi)$. The cost of this procedure is that it requires N function evaluations of the determinant in Eq. (2). However, this cost is unavoidable in order to guarantee that a zero of the function is not missed.

3.4 Beam model classes

Two families of model classes are introduced based on the Euler-Bernoulli beam theory. The objective is to examine which of the introduced model classes are most appropriate to model the hanger and produce reliable estimates of the hanger tension. Model class *Bfix* is the beam model with fixed ends, while model class *Bflex* is a beam model with flexible ends simulated by rotational springs, two at each side of the beam. For the three-dimensional beam, the vibrations of the beam in the (x, z) and (y, z) planes are considered uncoupled for both model classes. Thus, for a given value of ξ, the modal frequencies are computed by solving 2 two-dimensional beam problems, considering the boundary conditions for each plane motion, one in the (x, z) plane with spring constants k_1, k_3 and the other in the (y, z) plane with spring constants k_2, k_4.
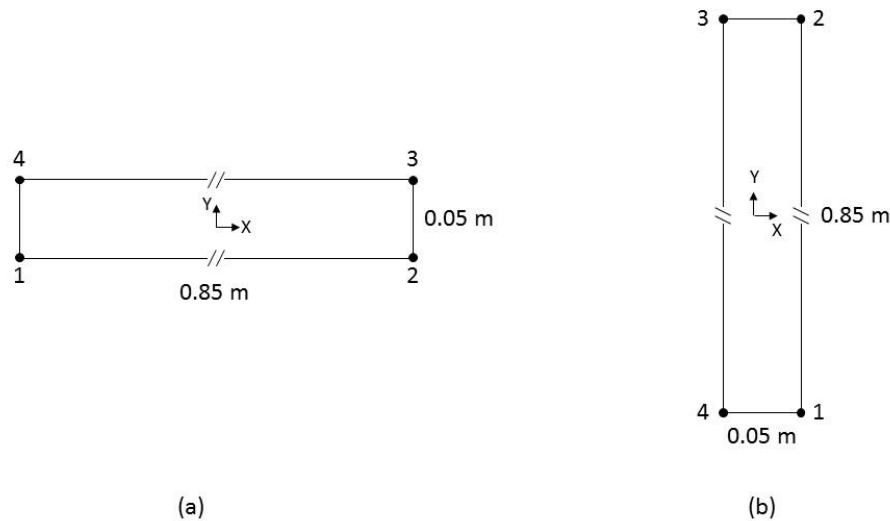
Fig. 5 Plate surface connecting with (a) deck (bottom edge of hanger), and (b) arch (top edge of hanger)

The concept of effective length (Bellino, Marchesiello *et al.* 2010) is also introduced to take into account the flexibility of the end conditions. Beam models with either one or two effective lengths (one per direction of deflection) are used to account for the different flexibilities per direction of the end connections due to different orientation of the connecting plate at the bottom and top of the hanger and the unknown boundary conditions arising from the deck and arch flexibility. The model classes are flexible to predict different modal frequencies along the transverse and longitudinal direction of the beam by using different effective lengths per direction of hanger deflection and/or applying different rotational spring constants. Each one of the introduced families of model classes contain models that are further classified in Section 6 depending on the number and type of parameters they include for estimation.

4. Modal frequency predictions based on finite element models

A high fidelity FE model is also used to predict the modal frequencies of the hanger shown in Fig. 2, under different boundary conditions. The FE modeling and analyses are carried out using the ABAQUS general purpose FE program. Second-order ten-node tetrahedral elements (C3D10) are used to create the FE mesh in the 10 m beam with circular cross-section, as well as in the two $1m$ end plate connections of the circular beam with the rest of the bridge structure. The model consists of about 71,500 nodes, 43,000 elements, and a total of 215,000 nodal DOF. Mesh sensitivity studies were carried out to select the optimal mesh size that ensures convergent numerical calculations providing accurate predictions of the lowest 12 modal frequencies.

4.1 Types of boundary conditions and FE model classes

Two different types of boundary conditions are considered. The first type corresponds to fixed ends at the boundaries, implemented by constraining the motion of the DOFs at the bottom and top plate surfaces (Fig. 5), connecting with the deck and the arch, to be zero. The fixed-end finite element model is denoted by *FEfix* and involves the hanger tension as parameter to be estimated using the measured data. The second type permits only the rotation of the bottom and top plate surfaces (connecting with the deck and the arch) about the two axes x and y along the longitudinal and transverse directions of the bridge deck, respectively. These boundary conditions are implemented by constraining the motion of the midpoint of the boundary plate surface to zero along all three x, y and z directions, constraining the movement of the side nodes of the edge surface along the x and y directions to zero, and adding springs along the z direction of the side nodes of the edge surface, restraining their motion along the z direction of the hanger according to the spring constants. Such springs provide resistance to rotations of the edge surfaces with respect to the x and y axes.

Two independent sets of springs are added to simulate the rotational resistance with respect to the x and y axes. Each set is uniformly distributed along the opposite sides of the edge surface. The distributed stiffness values are denoted by $k_{rx,b} = k_1$ for the springs along the sides 1-2 and 3-4 of the bottom edge surface (Fig. 5(a)), $k_{rx,t} = k_3$ for the springs along the sides 2-3 and 4-1 of the top edge surface (Fig. 5(b)), $k_{ry,b} = k_2$ for the springs along the sides 2-3 and 4-1 of the bottom edge surfaces (Fig. 5(a)), and $k_{ry,t} = k_4$ for the springs along the sides 1-2 and 3-4 of the top edge surfaces (Fig. 5(b)). The flexible end FE model is denoted by *FEflex* and involves five parameters to be estimated using the measured data: the hanger tension and the four distributed spring constants k_1, k_2, k_3 and k_4.

4.2 Estimation of modal frequencies

The high tension of the hanger affects the modal frequencies due to increase in the tangent stiffness. In order to predict the tangent stiffness due to hanger tension and subsequently the effect on the modal frequencies of the hanger, a geometrically nonlinear analysis of the hanger has to be performed. The evaluation of the modal frequencies in Abaqus that takes into account the stiffness increase due to large hanger tension consists of a certain sequence of actions. The aim is to obtain the modal frequencies of the system after the hanger tension has been applied.

Action 1: This is a static deformation step for estimating the tangent stiffness matrix under the application of the hanger tension. The hanger tension is applied at one edge (e.g., bottom edge in Fig. 5(a)). The boundary conditions at the bottom edge are deactivated to allow the hanger to deform. The axial load T is applied as a pressure $p = T / (bh)$ uniformly distributed through the bottom face of the connection. The geometrically nonlinear static analysis is performed and the tangent stiffness matrix and the mass matrix are then extracted from the Abaqus model.

Action 2: After the hanger has been elongated in Action 1, the correct boundary conditions are activated at the bottom edge and the hanger is kept in its deformed state. Specifically, for fixed-end

hanger conditions, all displacement DOFs at the bottom edge of the hanger are restrained. For flexible supports, springs are added at the bottom edge DOFs so that rotational stiffness conditions are simulated. The resulting mass matrix as well as the stiffness matrix which consist of the tangent stiffness matrix and the stiffness due to the spring constants is extracted from Abaqus.

Action 3: Using the mass matrix and the tangent stiffness matrix obtained from Action 2, the eigenvalue analysis is performed to obtain the modal frequencies and the mode shapes of the hanger. It should be noted that due to the non-circular cross-section of the hanger along its total length, arising from the 1m plate connections, a mode shape deforms both in (x, z) and (y, z) planes, in contrast to the in-plane deformation predicted by the Euler-Bernoulli beam theory when circular cross-section is assumed. The mode shapes are used to distinguish the type of the closely spaced modes by monitoring the mode shape deformation in the (x, z) and the (y, z) planes. In this way mode switching which may happen as the hanger tension varies in the Bayesian inverse formulation outlined in Section 5 can be monitored so that the correct modes with dominant hanger deflection in the longitudinal or transverse direction of the bridge are associated to the experimentally identified modes.

5. Bayesian inference

The Bayesian framework for parameter estimation and model selection (Beck and Katafygiotis 1998, Yuen 2010, Simoen, Moaveni *et al.* 2013, Vanik, Beck *et al.* 2000) is used to estimate the hanger axial load based on the model classes introduced in the previous sections. The inference is based on the lowest m experimentally identified modal frequencies $D = \{\hat{\omega}_r, r = 1, ..., m\}$ of the hanger. Consider a parameterized model class M and let $\underline{\theta} \in R^{N_\theta}$ be the set of free structural model parameters to be identified. Depending on the model class used, the model parameters may include the hanger force, the equivalent beam length(s) and the rotational stiffness of the boundary conditions of the hanger. Let also $\omega_r(\underline{\theta})$ be the predictions of the modal frequencies obtained for a particular value of the parameter set. These modal frequencies conditioned on the values of the model parameters are computed as outlined in Sections 3 and 4 for the analytical and computational models, respectively.

Probability density functions (PDF) are used to quantify uncertainties in the parameter set $\underline{\theta}$. Using Bayes' theorem, the posterior PDF $p(\underline{\theta} | D, M)$ of the model parameters $\underline{\theta}$ based on the measured data D and the modeling assumptions M, is obtained as follows

$$p(\underline{\theta} | D, M) = \frac{p(D | \underline{\theta}, M) p(\underline{\theta} | M)}{p(D | M)} \tag{18}$$

where $p(D | \underline{\theta}, M)$ is the probability of observing the data (likelihood function) from a model M corresponding to a particular value of the parameter set $\underline{\theta}$, $p(\underline{\theta} | M)$ is the prior PDF of the model parameters, and $p(D | M)$ is the evidence of the model class given by

$$p(D | M) = \int_\Theta p(D | \underline{\theta}, M) p(\underline{\theta} | M) d\underline{\theta} \tag{19}$$

where Θ is the domain of variation of the model parameters.

The likelihood $p(D|\underline{\theta},M)$ is derived by using a probability model for the prediction error e_r, $r=1,\ldots,m$, for the modal frequencies defined as the fractional difference between the measured modal frequencies and the corresponding modal frequencies predicted from the model class M using a particular value of the parameter set $\underline{\theta}$. Specifically, e_r satisfies the prediction error equation

$$\hat{\omega}_r = \omega_r(\underline{\theta}) + \omega_r e_r \tag{20}$$

for all modes $r=1,\ldots,m$. Modeling the prediction errors as zero-mean Gaussian variables, $e_r \sim N(0,\sigma^2)$, with standard deviation σ, assuming that the prediction errors are independent, and including the prediction error parameter σ into the uncertain parameter set $\underline{\theta}$, the likelihood $p(D|\underline{\theta})$ takes the form

$$p(D|\underline{\theta},M) \sim \frac{1}{(\sqrt{2\pi})^m \sigma^m} exp\left[-\frac{m}{2\sigma^2}J(\theta)\right] \tag{21}$$

where $J(\underline{\theta})$ given by

$$J(\underline{\theta}) = \frac{1}{m}\sum_{r=1}^{m}\frac{[\omega_r(\underline{\theta}) - \hat{\omega}_r]^2}{[\hat{\omega}_r]^2} \tag{22}$$

represents the measure of fit between the measured modal frequencies and the modal frequencies predicted by the model.

The Bayesian framework can also be used to select the best model class among a family of alternative competitive model classes $M_1,\ldots,M_\mu$ (Beck and Yuen 2004), used to represent the dynamics of the hanger. Using the Bayes theorem, the posterior probability $P(M_i|D)$ of the model class M_i given the data D is obtained from

$$P(M_i|D) = \frac{p(D|M_i)P(M_i)}{p(D)} \tag{23}$$

where $p(D|M_i)$ is the evidence of M_i, $P(M_i)$ is the prior probability of M_i and $p(D) = \sum_{i=1}^{\mu} p(D|M_i)P(M_i)$ is a normalizing constant that guaranties that the sum of the probabilities over all model classes considered in the selection equals one. Assuming that the model classes are equally probable prior to the use of the data, then the most probable model class based on the data corresponds to the model class with the highest evidence.

Bayesian computational tools are used to estimate the uncertainty in the model parameters, select the best model class and propagate uncertainty. Herein we use the TMCMC (Ching and Chen 2007) and its parallelized extended version (Angelikopoulos, Papadimitriou *et al.* 2012) in order to sample from the posterior PDF of each model class, estimate uncertainties in the model parameters such as axial hanger load and equivalent length(s), as well as propagate uncertainties to compute output quantities of interest such as modal frequencies. One more merit of using the TMCMC algorithm for Bayesian purposes is the calculation of the evidence as a by-product of the algorithm (Ching and Chen 2007). Note that for identifiable cases, the Gaussian approximation of the posterior PDF of the model parameters (Yuen and Mu 2011, 2015) can also be used to save

computational effort for the hanger problem. This usually requires the availability of the first and second derivatives of the minus the logarithm of the posterior PDF with respect to the model parameters. However, analytical formulations for such derivatives based on direct differentiation or adjoint methods are not readily available and such approximate formulation has not being pursued further in this work. Instead the TMCMC is very suitable for the considered model classes due to the model non-intrusiveness and the absence of analytical derivatives of the output quantities of interest with respect to model parameters (Hadjidoukas, Angelikopoulos *et al.* 2015). The most probable values of the parameters in $\underline{\theta}$ are also obtained by minimizing the $-\log p(\underline{\theta}|D,M)$ using the CMA-ES algorithm (Hansen, Muller *et al.* 2003).

6. Results

The axial load is estimated using the FE model classes and the simple beam model classes introduced in the previous sections. Estimation is based on the lowest twelve experimentally identified modal frequencies of the hanger (see Table 1), six along the transverse and six along the longitudinal direction of the bridge deck. The objective is to estimate the value of the hanger tension and its uncertainty, to explore the effect of the end hanger conditions and the number of measured modal frequencies on the accuracy of the hanger tension estimates, and to select the best model classes based on simplified beam theory that are adequate representations of the hanger behavior.

The parameter estimation and the model class selection is performed for the model classes reported in Table 3. The FE model classes *FEfix* and *FEflex* are used to identify whether or not the flexibility in the end conditions of the hanger, arising from the flexibility of the arch and the deck, is important. The simple beam model classes *Bfix* and *Bflex* are used for the purpose of identifying which one of them is capable of predicting adequately the hanger tension based on the results obtained from the FE model classes which are considered to contain the more accurate information for the hanger tension. Depending on the type and number of parameters they are left free to be inferred by the Bayesian formulation, the beam model classes are further classified as follows.

- *Bfix*(T, L) : two-parameter model class, with parameters the hanger tension T and the equivalent hanger length L. This model uses the equivalent length concept (Bellino, Marchesiello *et al.* 2010) so that it can adjust the length of the uniform cross-section of the beam to fit the modal frequency data, thus accounting for the flexibility of the end plate connections and the boundary conditions between the hanger and the arch or the deck.

- *Bfix*(T, L_t, L_l) : three-parameter model class, with parameters the hanger tension T and equivalent hanger lengths L_t and L_l assumed to be different for deflections in the (x, z) (longitudinal direction) and (y, z) (transverse direction) planes. This model has freedom to provide different beam flexibilities along the transverse and longitudinal directions of motion and thus better fit the different values of the experimental modal frequencies observed along these two directions (see Table 1).

- $Bfix(T \mid L_i)$: a family of μ one-parameter model classes with parameter the hanger tension given the value of the hanger length to be L_i, $i = 1, \ldots, \mu$. Each model class is defined by the different value L_i of the beam length. The aim is to choose the best model class or, equivalently, the best equivalent hanger length L_i that best represents the observed data.

A similar classification is introduced for *Bflex* model classes resulting in

- $Bflex(T, L, \underline{k})$: three- to six-parameter models, with parameters the hanger tension, the equivalent length, as well as the rotational stiffnesses at the two ends. The rotational stiffness to be included in $\underline{k}$ may vary from one to four. For example, $Bflex(T, L, k_1, k_3)$ denotes the model class with the rotational stiffness k_1 and k_3 (see Fig. 3) used as free parameters to be determined, while the k_2 and k_4 are set fixed to 10^{15} to simulate rigid supports at the respective directions.

The nominal value of the axial load is considered to be $T_0 = 922 KN$ corresponding to the most probable value of the fixed-end beam model based on the lowest two experimental frequencies, one in the transverse and the other in the longitudinal direction. The nominal value of the hanger length is L_0=12 m, corresponding to the total length that includes the approximately 2 m length of the plate connectors (Fig. 2) at the two ends. The parameters θ_T and θ_L in the set $\underline{\theta}$, introduced for the axial load T and the length L of the beam, respectively, scale the nominal values so that the axial load is $T = \theta_T T_0$ and the length is $L = \theta_L L_0$. The nominal values of the spring stiffnesses used to simulate boundary conditions are taken to be $k_{nom} = 10^{10}$. For a spring stiffness k, the corresponding parameter θ_k in the set $\underline{\theta}$ is introduced so that $k = (k_{nom})^\theta = 10^{10\theta_k}$.

The prior distributions of all parameters are selected to be uniform. The bounds are selected to be $\theta_T \in [0.5, 1.5]$ for the hanger tension parameter, $\theta_L \in [0.817, 1.2]$ for the length of the beam model, and $\theta_k \in [0.1, 1.5]$ for all the spring stiffness parameters. Note that the lower bound 0.817 for θ_L corresponds to the clear length $L_{cl} = 0.817 * 12 = 9.817$ m of the circular part of the hanger. The range of variation of the prediction error parameter σ is $\sigma \in [0.001, 0.1]$. The TMCMC algorithm (Ching and Chen 2007, Angelikopoulos, Papadimitriou *et al.* 2012) is used to sample the posterior PDF of each model class, compute the uncertainties in the model parameters, estimate the evidence of each model class, and propagate uncertainties to predictions of the modal frequencies. The values of the TMCMC parameters (Ching and Chen 2007) are selected to be $\beta^2 = 0.2$ and $TolCov = 1.0$. The most probable values of the model parameters are obtained using the CMA-ES algorithm (Hansen, Muller *et al.* 2003) with the search domain to be the one defined by the support of the uniform priors assumed for the model parameters.

Table 3 presents the most probable value (MPV), the mean, the standard deviation, and the 5%, 50% and 95% quantiles of the hanger tension estimated from all model classes. The number of samples per TMCMC stage is 1000 for *FEflex*, 500 for *FEfix*, 5000 for *Bfix* and *Bflex* model classes. The different number of samples per TMCMC stage used for each model class is

chosen as a trade-off between computational effort and solution accuracy. A large number of samples is used for the analytical beam model due to the small time-to-solution, of the order of a few minutes, in relation to the time-to-solution required for estimating the hanger force using the finite element model classes. A smaller number of 500 samples per TMCMC stage is used for the FEfix model class due to a small number of two parameters involved as opposed to six parameters involved in the FEflex model class. Representative times-to-solution obtained in a dual 4-core computer using the parallelized versions of TMCMC algorithm are of the order of 60 hours for *BEflex*, 12 hours for *BEfix* and several minutes for the *Bfix* and *Bflex* model classes. The number of TMCMC stages, which affect the time-to-solution is approximately 4 to 7, depending on the model class and the individual run.

6.1 Hanger force estimation based on FE model classes

Comparing the log evidence for the FE model classes *FEflex* and *FEfix* it can be seen that the *FEflex* is clearly the preferred model since the resulting relative probabilities of the two models are $Pr(FEflex|D) = a/(1+a) = 0.86$ and $Pr(FEfix|D) = 1/(1+a) = 0.14$, where $a = exp(24.03 - 22.24)$ is evaluated from the log evidence values in Table 3. The *FEflex* gives a significantly better fit to the data which is equal to 1.03% as compared to the fit 2.63% for the *FEfix* model. The two FE models give completely different predictions of the hanger tension. Model *FEflex* predicts the most probable value at 0.91 with uncertainty as quantified by the quantiles to be in the range [0.75,1.04] (std=0.090), while the *FEfix* predicts the most probable value to be 22% lower at 0.70 with uncertainty to be in the range [0.60,0.80] (std=0.063).

To identify the source of such differences the results of the models *FEfix(long)* and *FEfix(trans)* are used. The *FEfix(long)*, which is based on fitting the six modal frequencies with dominant hanger deflections along the longitudinal direction, give predictions of the hanger tension that are closer to those obtained by the *FEflex*. In contrast, the *FEfix(trans)* which is based on fitting the six modal frequencies with dominant hanger deflections along the transverse direction gives predictions that are approximately 35% lower than the *FEflex* model predictions and 15% lower than the *FEfix* model predictions. These differences in predictions are due to the fact that the experimentally identified modal frequencies of the hanger in the transverse direction are consistently lower than the modal frequencies of the hanger in the longitudinal directions (see Table 1) which, due to the symmetry of the hanger and the orientation of the top and bottom identical plate connections in the transverse and longitudinal directions, it can only be explained by the flexibility of the arch and/or the deck when the hanger vibrates in the transverse direction. This support flexibility was accounted in the model class *FEflex* while in the model class *FEfix(trans)* it was ignored resulting in a significantly lower hanger tension in order to compensate and match the lower modal frequencies. The *FEfix* models class which did not allow for support flexibility in both directions also resulted in lower hanger tension, trading-off the fit of the modal frequencies in the longitudinal and transverse direction.

The most probable values of the rotational stiffnesses are estimated from the *BEflex* model class to be $k_1 = 10^8$, $k_2 = 10^{11}$, $k_3 = 10^4$ and $k_4 = 10^{13}$, with the value of k_3 being significantly smaller than the other 3 much stiffer rotational springs, indicating that the main

source of support flexibility is at the top end of the hanger in the transverse direction and it is due to the flexibility of the bridge arch. In conclusion, the 5-parameter model *FEflex* is the most preferred model class as compared to the one-parameter *FEfix* model class and predicts more reliably the hanger force, while the *FEfix* underestimates the hanger force by approximately 22%·

From the values of the standard deviation and the 5% and 95% quantiles of the hanger tension predicted from the *FEflex* model, it can also be concluded that the uncertainty in the hanger tension is of the order of 10%. This uncertainty is due to the inability of the model class *FEflex* to fit exactly all 12 modal frequencies. This uncertainty in the hanger force prediction should be taken into account when using the values of the hanger tension to infer structural safety. In contrast to existing studies that report a single value of the hanger force, the Bayesian inference framework also estimates the uncertainty in such a value. This uncertainty may affect the safety margins of the hanger and the bridge. From the engineering point of view, using the nominal hanger tension value of $T_0 = 922 KN$ and the hanger cirular cross-sectional area of diameter D=0.130 m, one has that the stress prediction in the hanger within 5% and 95% credible intervals ranges between $[0.16, 0.22]\sigma_y$ values, where $\sigma_y = 330 MPa$ is the yield stress of this specific hanger, resulting in a relative high safety factor (well within the safe domain when failure is assumed to occur due to stresses in the hanger exceeding material yield or fracture stresses).

6.2 Hanger force estimation based on simple beam model classes

The ability of the simplified beam model classes to predict the hanger tension is next examined. From the results in Table 3 it can be observed that almost all simplified beam models make predictions of the value of the hanger tension and its uncertainty that are significantly closer to the predictions of the *FEflex* model than the predictions of the *FEfix* model. This is very promising for using such simplified models for hanger tension predictions.

Comparing the log evidence values for the fixed support model classes $Bfix(T, L)$ and $Bfix(T, L_t, L_l)$, it can be clearly seen that the 3-parameter model class $Bfix(T, L_t, L_l)$ has higher preference than the two-parameter model class $Bfix(T, L)$ with $Pr(Bfix(T, L_t, L_l) | D) = 0.85$ and $Pr(Bfix(T, L) | D) = 0.15$. The error for the most probable parameter values (last column in Table 3) obtained by CMA is 1.1% for the $Bfix(T, L_t, L_l)$ model which should be compared to the 2.6% error for the $Bfix(T, L)$ model. Both models provide a sample mean estimate of the hanger force which is approximately 5% less than the mean estimate of the *FEflex* model class. The 5% and 95% credible intervals quantifying the uncertainty in the hanger force are predicted by both beam models to be close to the corresponding uncertainty bounds predicted by the *FEflex*, with the $Bfix(T, L)$ to slightly underestimate the lower bound, while the $Bfix(T, L_t, L_l)$ to slightly underestimate the upper bound.

To assess the correlation between the hanger tension and the equivalent beam length, the projection of the posterior samples obtained using the TMCMC algorithm in the two-dimensional space (θ_T, θ_L) of the model parameters is presented in Fig. 6 for the model class $Bfix(T, L)$. We note that the length of the beam has a positive correlation with the axial load of the beam which is expected since when the length is increased, the frequencies tend to decrease. As a result the

hanger tension and thus the predicted modal frequency must be increased to compensate this decrease, maintaining the fit with the values of the experimental modal frequencies.

Table 3 Log evidence and estimates of hanger tension for all model classes

| Model class	N_θ	Log Evidence	Tension quantiles [5%, 50%, 95%]	Tension Mean	Tension Standard Dev.	Tension MPV	Fit
FEflex	5	24.03	[0.75, 0.92, 1.04]	0.909	0.0897	0.822	0.0103
FEfix	1	22.24	[0.59, 0.70, 0.80]	0.701	0.0627	0.701	0.0263
FEfix(long)	1	–	[0.75, 0.83, 0.92]	0.836	0.0498	0.831	0.0102
FEfix(trans)	1	–	[0.52, 0.60, 0.75]	0.616	0.0714	0.576	0.0237
Bfix(T,L)	2	20.72	[0.68, 0.86, 1.06]	0.867	0.114	0.854	0.0248
Bfix(T,L_t,L_l)	3	22.49	[0.73, 0.86, 0.98]	0.856	0.0731	0.856	0.0115
Bflex(T,L,k_3)	3	20.90	[0.70, 0.88, 1.08]	0.883	0.1215	0.888	0.0112
Bflex(T,L,k_1,k_3)	4	20.10	[0.70, 0.94, 1.35]	0.974	0.1905	0.888	0.0112
Bflex(T,L,$\underline{k}$)	6	19.23	[0.77, 1.19, 1.44]	1.144	0.2196	0.968	0.0115
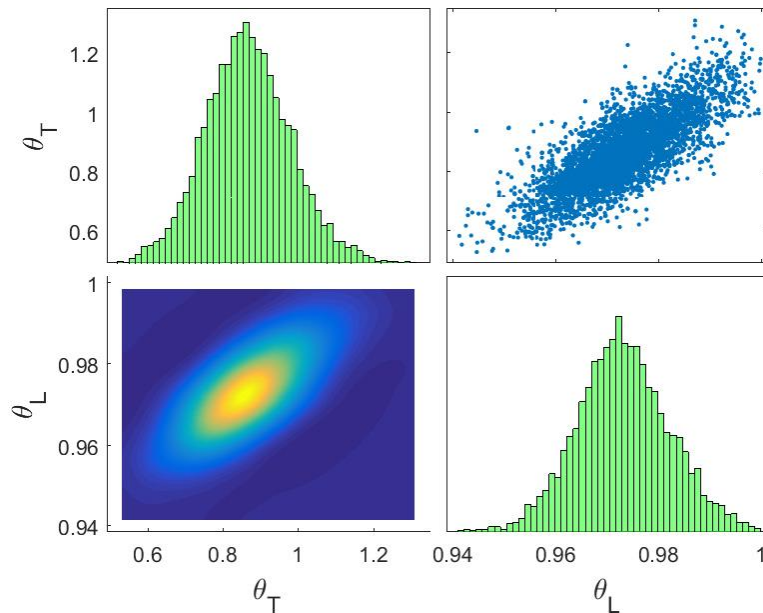
Fig. 6 Parameter estimation for model class *Bfix(T,L)*. Diagonal: Marginal distributions. Above-diagonal: sample projections in (θ_T,θ_L) parameter space. Below Diagonal: Contour plots in (θ_T,θ_L) parameter space

Concerning the flexible-end beam model classes $Bflex(T,L,k_3)$, $Bflex(T,L,k_1,k_3)$ and $Bflex(T,L,\underline{k})$, the log evidence values suggest that the least-parameter model class $Bflex(T,L,k_3)$ is preferred to the 4-parameter and 6-parameter model classes since the addition of the extra parameters in the model is penalized by the Bayesian formulation, considered it as overfitting (Beck and Yuen 2004). The 3-parameter model class $Bflex(T,L,k_3)$ provides reasonable uncertainty bounds of [0.70,1.08] of the hanger force, that are closer to the ones provided by the two-parameter model $Bfix(T,L)$, while the error in the fit is 1.1% which is closer to the error provided by the $Bfix(T,L_t,L_l)$ model. This means that the $Bflex(T,L,k_3)$ fits better the experimental data than the $Bfix(T,L)$ model. The models $Bflex(T,L,k_1,k_3)$ and $Bflex(T,L,\underline{k})$, which are less prefferred mainly due to overparameterization, predict much higher mean hanger tension and uncertainty bounds. This can be attributed to the flexibility that this model has to provide a reasonable fit to the data by trading-off the hanger force values with the flexibility of the springs at the end supports.

Comparing the $Bfix$ and $Bflex$ model classes, the most preferred model corresponding to the largest log evidence value is $Bfix(T,L_t,L_l)$ with the second and third preferred model classes to be $Bflex(T,L,k_3)$ and $Bfix(T,L)$, respectively. Comparing with the $FEflex$ model results, the most preferred $Bfix(T,L_t,L_l)$ model gives slightly tighter uncertainty bounds for the hanger force. The worst fit in the experimental frequencies is accomplished by the two-parameter $Bfix(T,L)$ model due to its less flexibility with a single equivalent hanger length to simultaneously fit the modal frequencies in the transverse and longitudinal directions. In contrast, model $Bflex(T,L,k_3)$ is flexible to simultaneously fit the longitudinal modal frequencies by adjusting the beam length, and the transverse modal frequencies by adjusting the spring stiffness k_3.

Table 4 presents the 5% and 95% quantiles, the mean and the standard deviation of the equivalent length estimated from each simple beam model class introduced in Table 3. It can be seen that the identified uncertainty in the equivalent length values is very narrow. Comparing the fixed-support model classes, $Bfix(T,L)$ gives uncertainty bound of $[0.959,0.988]L_0$, while $Bfix(T,L_t,L_l)$ gives lower values $[0.949,0.972]L_0$ for L_l and higher values $[0.972,995]L_0$ for L_t to make the beam more flexible to fit the lower modal frequencies in the transverse direction. The coefficient of variation (cov = standard deviation over mean) for the $Bfix(T,L)$ model is 0.9%, while for the $Bfix(T,L_t,L_l)$ model it is approximately 0.7% for both L_t and L_l. All these uncertainties are quite small compared to the uncertainty of 10% predicted for the hanger tension.

Fig. 7(a) presents the results of the estimation of the hanger force by using the family of models $Bfix(T \mid L_i)$ with L_i varying within the uncertainty bound computed by the $Bfix(T,L)$ model. Fig. 7(b) gives the evidence of each model in the family. It is clear that the best model class is the one that corresponds to length $L_{best} = 0.973$ and predicts hanger tensions that are consistent with the ones predicted by $Bfix(T,L_t,L_l)$, with narrower uncertainties since it does not take into account the uncertainty in the equivalent length. However, as one moves away from the best values of the equivalent length, the predictions of hanger tension values and uncertainties depart considerably (underpredicting or overpredicting) from the predictions of the baseline FE model $FEflex$ or $Bfix(T,L_t,L_l)$. This means that arbitrary guesses of the equivalent length to carry out

the identification of the hanger tension are highly likely to give erroneous estimates. The proposed Bayesian method is a rational framework to provide the correct estimates of the hanger tension and equivalent lengths, as well as their uncertainties.

Finally, the estimates of the equivalent length L provided by the $Bflex(T,L,k_3)$ model are closer and slightly larger than the estimates of L_l for the $Bfix(T,L_t,L_l)$ model so that the experimentally identified longitudinal modal frequencies are matched, while the stiffness k_3 of the $Bflex(T,L,k_3)$ model is adjusted to match the modal frequencies in the transverse direction. The uncertainty in the equivalent length L values is higher (cov= 1.0%). The uncertainties in the equivalent length L predicted by the four parameter model $Bflex(T,L,k_1,k_3)$ and the seven-parameter model $Bflex(T,L,\underline{k})$ are even higher (1.5% and 1.9%, respectively), due to the flexibility of these models to compensate the change in the equivalent length by a change in the rotational stiffness values in order to fit the identified modal frequencies. In any case even the highest uncertainty of 1.9% is small, indicating the narrow range of values that the equivalent length can take in order to fit the measured data.

Fig. 8 presents the propagation of the uncertainty in the model parameters to the lowest twelve modal frequencies. The results in this Figure correspond to predicted modal frequencies normalized with respect to the experimental frequencies. Thus the distance of these values from one is a measure of how close the values of the model predicted modal frequencies are to the experimentally identified modal frequencies. We can clearly see the impact of the flexible end supports of the *FEflex* model in predicting the modal frequencies compared to the fixed-end model class *FEfix*. The fixed-end FE model class cannot reliably predict the measured modal frequencies, missing at least seven of them by as much as 4%. The flexible-end FE model class reliably predicts all measured modal frequencies, since the line equal to 1 is within the uncertainty bounds of the predictions for most modal frequencies. We also notice that the 3-parameter beam model classes $Bfix(T,L_t,L_l)$ and $Bfix(T, L, k_3)$ also give good predictions of the modal frequencies.

Table 4 Estimates of the hanger equivalent length for all beam model classes

Model class	Length quantiles [5%, 50%, 95%]	Length Mean	Length Standard Dev.
$Bfix(T,L)$	[0.959, 0.973, 0.988]	0.975	0.0090
$Bfix(T,L_t,L_l) - L_t$	[0.972, 0.984, 0.995]	0.984	0.0070
$- L_l$	[0.949, 0.960, 0.972]	0.960	0.0071
$Bflex(T,L,k_1)$	[0.953, 0.970, 0.986]	0.970	0.0101
$Bflex(T,L,k_1,k_2)$	[0.938, 0.965, 0.985]	0.964	0.0138
$Bflex(T,L,\underline{k})$	[0.923, 0.950, 0.980]	0.951	0.0178

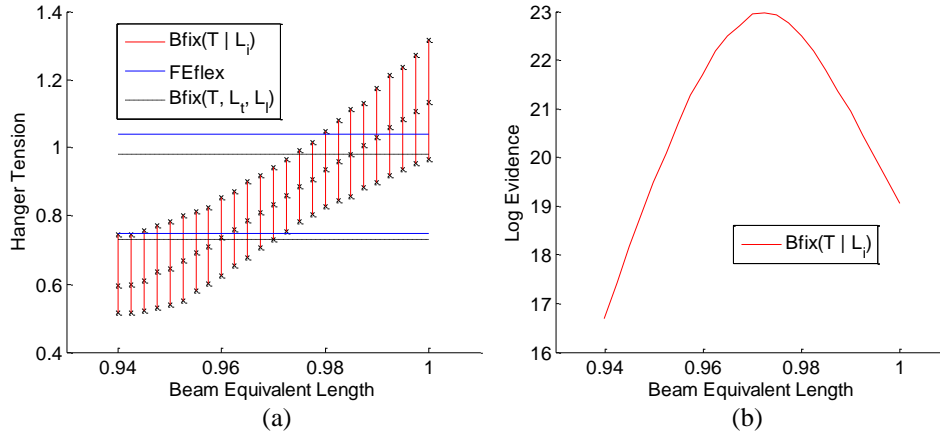Fig. 7 (a) Comparison of hanger tension 5%, 50% and 95% quantiles estimated by the model classes $Bfix(T|L_i)$ with 5% and 95% quantiles estimated by the model classes $FEflex$ and $Bfix(T,L_t,L_l)$. (b) Log evidence values of model classes $Bfix(T|L_i)$ for different L_i values

The predictions of the $Bfix(T,L_t,L_l)$ model class based on the two equivalent lengths, independent in the transverse and longitudinal directions, give very similar predictions of the modal frequencies and their uncertainties to those obtained from the $FEflex$ model class for several of the modal frequencies. The $Bfix(T,L,k_3)$ also gives similar predictions but with higher uncertainty. The predictions of the 2-parameter model class $Bfix(T,L)$ are closer to those of the fixed-end $FEfix$ model than to $FEflex$ model, with much higher uncertainty so that a number of measured modal frequencies are contained within the uncertainty bounds. From the simple beam model classes, the best predictions are obtained from model class $Bfix(T,L_t,L_l)$.

To study the effect of the number of modal frequencies used in the identification, Fig. 9(a) presents results for the hanger force (mean and quantiles values) estimated from the model classes $Bfix(T,L)$, $Bfix(T,L_t,L_l)$ and $Bflex(T,L,k_3)$ using the lowest $m=4$ or 8 or 12 identified modal frequencies. Given m modal frequencies, $m/2$ correspond to the longitudinal direction and $m/2$ to the transverse direction. Results are also compared to the hanger force mean and quantile values estimated by the $FEflex$ model class. Similar results for the effective length mean and quantile values are presented in Fig. 9(b). We can clearly see the impact of the number of modes on the predictions of the hanger force uncertainties and structural reliability. As the number of modes used in the Bayesian identification decreases from 12 to 8 or 4, the uncertainty in the hanger tension and equivalent length values increases substantially for all beam model classes. This uncertainty increase is due to inadequacy of the small number of measured modal frequencies to identify with certainty the hanger tension and the equivalent lengths. When the hanger tension uncertainty is further used for structural safety estimation, the smaller number of measured modes leads to less reliable estimates of structural safety corresponding to higher failure probability than it is actually obtained from the identification that is based on a higher number of measured modal frequencies.
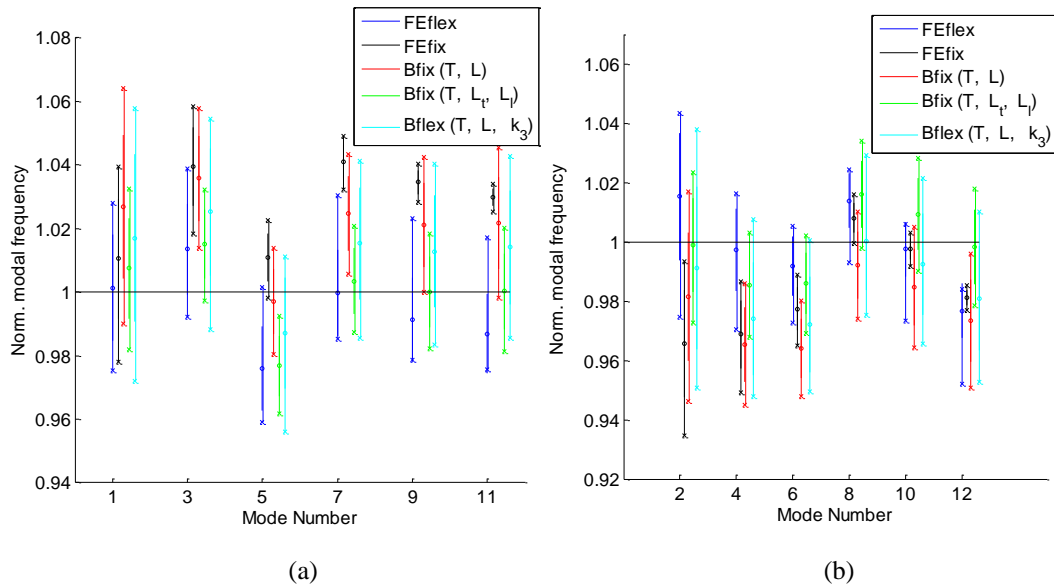
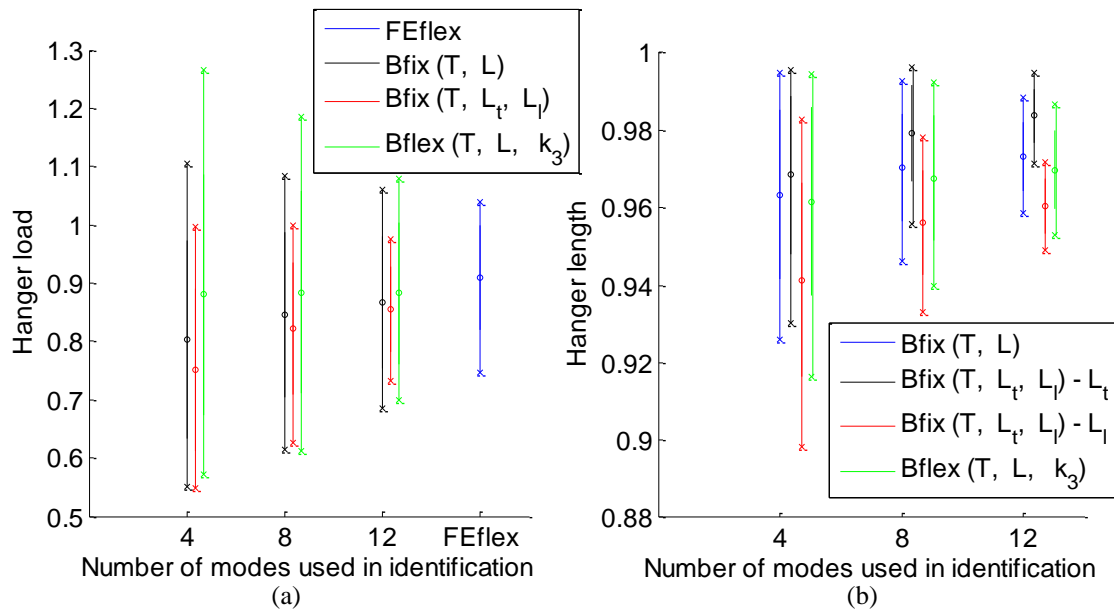Fig. 8 Uncertainty propagation to the output frequencies for selected model classes

Fig. 9 (a) Hanger tension mean and $[5\%, 95\%]$ quantiles and (b) hanger equivalent length mean and $[5\%, 95\%]$ quantiles for different model classes for 4, 8 and 12 modes used for identification

7. Conclusions

Bayesian inference is used to quantify and calibrate the uncertainties in the tension of bridge hangers by integrating the information from a structural model and the experimentally identified modal frequencies. A number of competitive structural model classes used for representing the vibrational characteristics of hangers are investigated for their accuracy, including simple Euler-Bernoulli beam models as well as high-fidelity FE models. The effect of the hanger end connection details and boundary conditions due to flexibility of arch and deck substructures on the hanger tension predictions is examined.

The high fidelity FE model with flexible supports, expected to give the most reliable estimates, is able to predict the lowest 12 experimentally identified modal frequencies in both transverse and longitudinal directions. The uncertainty in the hanger force is of the order of 10% of its mean value and should be taken into account in structural safety considerations. The FE model with fixed supports fails to fit the experimentally identified modal frequencies, underpredicting the hanger tension value and its uncertainty by more than 20%. Results suggest that the connection details and boundary conditions due to the flexibility of deck and arch substructures affect significantly the dynamics of the considered hanger. The flexibility arises mainly from the flexibility of the arch due to transverse deflections of the hanger.

The dynamics of the hanger in the longitudinal and transverse directions of the bridge seem to be reasonably approximated by simplified beam models using the concept of two independent equivalent lengths in the transverse and longitudinal direction, with values left free to be estimated by the Bayesian approach. The fixed-end beam model with the two independent equivalent lengths is selected by the Bayesian framework as the most preferred model class. It provides accurate estimates of the hanger tension and the uncertainties, close to the ones provided by the baseline FE model with flexible supports. The beam model with a single equivalent length fails to give adequate estimates of the measured modal frequencies for the specific hanger due to different modal frequencies arising from the asymmetry of the boundary conditions. The simplified beam model with a single equivalent length and end rotational springs is able to adequately represent the dynamics of the hanger, giving fairly accurate results with higher uncertainty in the values of the hanger tension, an indication that the model is less preferred than the fixed-end model with two equivalent lengths. A model with fixed length value selected arbitrarily is highly unlikely to fit the measured frequency data due to the fact that the dynamics of the beam is significantly affected by the selected value of the length of the beam. There is only a very narrow range of length values that fit the measured modal frequencies and give accurate predictions of the hanger tension.

The use of equivalent length and/or rotational springs to simulate hanger support flexibilities is deemed important in the beam modeling. Results suggest that the fixed-end models are substantially less accurate than the ones that take flexibility into account, either in terms of two equivalent lengths introduced to independently model flexibilities in transverse and longitudinal directions or in terms of a combination of an equivalent length and rotational springs. The Bayesian approach applied on the simplified beam models provides sufficiently accurate estimates of the hanger tension and its uncertainty, requiring three orders of magnitude less computational effort than the high-fidelity FE models. As the number of available identified modal frequencies increases, the prediction accuracy of the simple beam models is improved, while the uncertainty in the hanger tension is reduced. In contrast to inverse methods based on estimating a single value of the hanger tension, it is demonstrated in this study that the uncertainties in the hanger tension can

be significant and should be considered in inverse methods since they affect predictions of structural reliability and safety.

Acknowledgements

References

Angelikopoulos, P., Papadimitriou, C. and Koumoutsakos, P. (2012), "Bayesian uncertainty quantification and propagation in molecular dynamics simulations: A high performance computing framework", *J. Chem. Phys.*, **137**(14), 455-461.

Barcilon, V. (1976), "Inverse problem for a vibrating beam", *J. Appl. Math. Phys.*, **27**, 347-358.

Beck, J.L. and Katafygiotis, L.S. (1998), "Updating models and their uncertainties. I: Bayesian statistical framework", *J. Eng. Mech. - ASCE*, **124**(4), 455-461.

Beck, J.L. and Yuen, K.V. (2004), "Model selection using response measurements: Bayesian probabilistic approach", *J. Eng. Mech. - ASCE*, **130**(2), 192-203.

Belleri, A. and Moaveni, B. (2015), "Identification of tensile forces in tie rods with unknown boundary conditions", *Proceedings of the 7th International Conference of Inteligent Infrastructure SHMII*, July 1-3, 2015, Torino, Italy.

Bellino, A., Garibaldi, L., Fasana, A. and Marchesiello, S. (2011), "Tension estimation of cables with different boundary conditions by means of the added mass technique", *International Conference of Surveilance 6*, Oct. 25-26, 2011, University of Technology of Compiegne, France.

Bellino, A., Marchesiello, S., Fasana, A. and Garibaldi, L. (2010), "Cable tension estimation by means of vibration response and moving mass technique", *Mecanique et Industries*, **11**, 505-512.

Bokaian, A. (1990), "Natural frequencies of beams under tensile axial loads", *J. Sound Vib.*, **142**, 481-498.

Ceballos, M.A. and Prato, C.A. (2008), "Determination of the axial force on stay cables accounting for their bending stiffness and rotational end restraints by free vibration tests", *J. Sound Vib.*, **317**, 127-141.

Ching, J. and Chen, Y.C. (2007), "Transitional Markov chain Monte Carlo method for Bayesian model updating, model class selection, and model averaging", *J. Eng. Mech. - ASCE*, **133**(7), 816-832.

Ewins, D.J. (2000), *Modal Testing: Theory, Practice and Application*, Second edition, Research Studies Press Ltd., Baldock, England.

Fang, Z. and Wang, J.Q. (2012), "Practical formula for cable tension estimation by vibration method", *J. Bridge Eng. - ASCE*, **17**(1), 161-164.

Hadjidoukas, P.E., Angelikopoulos, P., Papadimitriou, C. and Koumoutsakos, P. (2015), "Π4U: A high performance computing framework for Bayesian uncertainty quantification of complex models", *J. Comput. Phys.*, **284**(1), 1-21.

Hansen, N., Muller, S.D. and Koumoutsakos, P. (2003), "Reducing the time complexity of the derandomized evolution strategy with covariance matrix adaptation (CMA-ES)", *Evolutionary Comput.*, **11**(1), 1-18.

Heylen, W., Lammens, S. and Sas, P. (1995), *Modal Analysis Theory and Testing*, Department of Mechanical Engineering, Katholieke Universiteit Leuven, Leuven, Belgium.

Huang, Y.H., Fu, J.Y., Wang, R.H., Gan, Q. and Liu, A.R. (2015), "Unified practical formulas for vibration-based method of cable tension estimation", *Adv. Struct. Eng.*, **18**(3), 405-422.

Humar, J.L. (2001), *Dynamics of Structures*, A.A. Balkema.

Kim, B.H. and Park, T. (2007), "Estimation of cable tension force using the frequency-based system

identification method", *J. Sound Vib.*, **304**, 660-676.

Lagomarsino, S. and Calderini, C. (2005), "The dynamical identification of the tensile force in ancient tie-rods", *Eng. Struct.*, **27**, 846-856.

Nam, H. and Nghia, N.T. (2011), "Estimation of cable tension using measured natural frequencies", *Procedia Eng.*, **14**, 1510-1517.

Ni, Y.Q., Ko, J.M. and Zheng, G. (2010), "Dynamic analysis of large diameter sagged cables taking into account flexural rigidity", *J. Sound Vib.*, **257**, 301-319.

Park, K.S., Seong, T.R. and Noh, M.H. (2015), "Feasibility study on tension estimation technique for hanger cables using the FE model-based system identification method", *Hindawi Publishing Corporation, Mathematical Problems in Engineering*, Volume **2015**, Article ID 512858, 12 pages.

Ren, W.X., Chen, G. and Hu, W.H. (2005), "Empirical formulas to estimate cable tension by cable fundamental frequency", *Struct. Eng. Mech.*, **20**(3), 363-380.

Simoen, E., Moaveni, B., Conte, J.L. and Lombaert, G. (2013), "Uncertainty quantification in the assessment of progressive damage in a 7-story full-scale building slice", *J. Eng. Mech. - ASCE*, **139**(12), 1818-1830.

Vanik, M.W., Beck, J.L. and Au, S.K. (2000), "Bayesian probabilistic approach to structural health monitoring", *J. Eng. Mech. - ASCE*, **126**(7), 738-745.

William, T.T. (1996), *Theory of Vibration With Applications*, CRC Press.

Yuen, K.V. (2010), *Bayesian Methods for Structural Dynamics and Civil Engineering*, Wiley.

Yuen, K.V. and Mu, H.Q. (2011), "Peak ground acceleration estimation by linear and nonlinear models with reduced order Monte Carlo simulation", *Comput. - Aided Civil Infrastruct. Eng.*, **26**(1), 30-47.

Yuen, K.V. and Mu, H.Q. (2015), "Real-time system identification: an algorithm for simultaneous model class selection and parametric identification", *Comput. - Aided Civil Infrastruct. Eng.*, **30**(10), 785-801.

Zui, H., Shinke, T. and Namyuita, Y. (1996), "Practical formula for estimation of cable tension by vibration method", *J. Struct. Eng. - ASCE*, **122**(6), 651-656.